Calculations of cross sections of resonant two-photon transitions to the second excited 4f5d state in Pr^{3+}:$Y_3Al_5O_{12}$ using density matrix theory

1999 J. Phys.: Condens. Matter 11 8177

(http://iopscience.iop.org/0953-8984/11/42/301)

J. Phys.: Condens. Matter **11** (1999) 8177–8184. Printed in the UK PII: S0953-8984(99)01245-X

Calculations of cross sections of resonant two-photon transitions to the second excited 4f5d state in Pr^{3+}:$Y_3Al_5O_{12}$ using density matrix theory

Zhenwen Dai†§, Jingyao Liu‡ and Siyuan Zhang†‖

† Laboratory of Chemistry and Physics of Rare Earth, Changchun Institute of Applied Chemistry, Chinese Academy of Sciences, Changchun 130022, People's Republic of China
‡ State Key Laboratory of Theoretical and Computational Chemistry, Jilin University, Changchun 130023, People's Republic of China

Received 25 January 1999, in final form 1 June 1999

Abstract. The density matrix resonant two-photon absorption (TPA) theory applicable to laser crystals doped with rare earth ions is described. Using this theory, resonant TPA cross sections for transitions from the ground state to the second excited state of the 4f5d configuration in Pr^{3+}:$Y_3Al_5O_{12}$ are calculated. The peak value of TPA cross section calculated is 2.75×10^{-50} cm^4 s which is very close to the previous experimental value 4×10^{-50} cm^4 s. The good agreement of calculated data with measured values demonstrates that the density matrix resonant TPA theory can predict resonant TPA intensity much better than the standard second-order perturbation TPA theory.

1. Introduction

Two-photon absorption (TPA) is a fundamental kind of frequency-upconverted process in laser crystals [1, 2]. Since the invention of the laser, studies of frequency-upconverted processes in laser crystals doped with trivalent or bivalent rare earth ions have never been discontinued [3–6]. Upconversion pumping may lead not only to the development of new laser schemes that cannot be excited through conventional optical pumping, but to obtain lasers at new and shorter wavelengths. In the last few years, therefore, more and more research have been carried out in exploration of upconversion mechanisms and upconversion lasing [7–10]. Smart *et al* [11] have reported frequency-upconverted visible lasers at room temperature in Pr^{3+} ion doped fluorozirconate fibre based on TPA processes in which two infrared pumping lights are used.

The trivalent praseodymium ion (Pr^{3+}) play a very important role in the understanding of optical and spectroscopic properties of rare earth impurity ion-activated insulators. What is more, for Pr^{3+} the broadband inter-configuration $4f^2 \rightarrow 4f5d$ transitions can offer the potential applications for tunable laser action at near ultraviolet wavelengths. Due to high-lying 4f5d energy levels as compared to those in the $4f^2$ configuration, it is difficult to realize $4f^2 \rightarrow 4f5d$ transitions in this ion by conventional light sources. Hence, the utilization of TPA pumping is an appropriate means of coping with this difficulty.

In order to give a more clear insight into the understanding of the properties of TPA processes in Pr^{3+} and other rare earth ions doped in laser crystals, characteristic physical

§ Permanent address: Department of Physics, Jilin University, Changchun 130023, People's Republic of China.
‖ Author for correspondence.

0953-8984/99/428177+08$30.00

quantities, such as TPA cross sections, are required. Gayen *et al* [12] measured some typical cross sections of resonant two-photon transitions from the ground state of the $4f^2$ configuration to the lowest state of the 4f5d configuration of Pr^{3+} in yttrium aluminium garnet, $Y_3Al_5O_{12}$ (YAG). In their following paper [13], they comprehensively measured resonant TPA cross sections for transitions from the ground state to the second excited state of the 4f5d configuration in Pr^{3+}:YAG when resonating the excitation energies with Stark levels of the ^3P_J ($J = 0, 1, 2$) and $^1I_6$ intermediate states. In addition, the peak cross section for non-resonant TPA of the lowest 4f $\rightarrow$ 5d near-ultraviolet transitions in Ce^{3+}:CaF_2 have also been estimated by Gayen and Hamilton [14]. Some cross sections of non-resonant TPA within the $4f^N$ configuration of Gd^{3+}:LaF_3 and Nd^{3+}:YAG/$LiYF_4$ were experimentally obtained by several groups [15–17]. Up to now, however, there is a scarcity of experimental cross section data for TPA of rare earth dopant ions in most laser crystals in common use. So, it is very significant to theoretically calculate them.

The standard second-order perturbation theory for two-photon transitions is described by Loudon [18]. Based on the Judd–Ofelt theory [19, 20], Axe [21] developed a second-order approximate method to evaluate the line strengths of intra-4f TPA transitions for rare earth ions. It has been demonstrated that Axe's theory can successfully explain the allowed TPA that obey the selection rules ($\Delta S = 0$, ΔL, $\Delta J \leqslant 2$) [17, 21, 22]. In principle, the sum of the intermediate states in the TPA theory includes all the electronic states of various configurations. Generally speaking, it is not possible to perform the complete sum over the intermediate states. For rare earth ions, the main intermediate states belong to the configurations $4f^N$ and $4f^{N-1}5d$ [17, 23]. This is certainly the case for the non-resonant TPA transition. For the resonant transitions, however, the resonant intermediate state can be taken as the only intermediate state because of its dominant contribution to the TPA processes. The second-order photon–electron interaction involving the resonant state will be much larger than the higher-order perturbation interactions. In the case of resonance, therefore, the frame of the second-order two-photon theory is adequate to describe the TPA intensities. This can be seen from [13] where a basic agreement between the theoretical and experimental cross sections of resonant f $\rightarrow$ d transitions in Pr^{3+}:YAG are obtained by Xie *et al* using the standard second-order TPA theory.

It can also be seen from [13] that there exists a discrepancy between the theoretical and experimental cross sections, i.e. that the experimental value is five times larger than the theoretical one for the TPA transition resonating with the intermediate state of the lowest Stark level of the $^3P_2$ state. In the present paper, we introduce the density matrix resonant TPA theory developed by Fujimura and Lin [24] and Lin *et al* [25] for molecular systems, and we present the means to apply this theory to laser crystals doped with rare earth ions. After that, by using this theory, we calculate resonant TPA cross sections, measured in the literature [13] by Xie *et al*, for transitions from the ground state to the second 4f5d state involving resonant Stark levels of the ^3P_J ($J = 0, 1, 2$) and $^1I_6$ intermediate states in Pr^{3+}:YAG. The density matrix resonant TPA theory is also a second-order perturbation theory. The purpose of this paper is to describe a more accurate second-order TPA theory, in which lattice vibration effects, such as the phonon frequency and the dimensionless displacement between transition states, of rare earth ions doped in laser crystals are considered.

2. Theoretical methods

Based on the density matrix theory in the Markoff approximation [25], the transition probability of TPA is separated into three terms: simultaneous, sequential and their mixing terms. In most cases the mixing term can be neglected. Therefore, the total transition probability W of TPA

equals the sum of the simultaneous term W_{sim} and sequential term W_{seq} as shown below. In the displaced harmonic oscillator model, the transition probability of the resonant TPA for a single vibrational mode in the low temperature limit can be expressed as [24]

$$\begin{aligned} W = W_{sim} + W_{seq} = {} & \frac{2|E_1|^2|E_2|^2|M_{nm}M_{ma}|^2}{\overline{h}^4}\exp[-(\Delta_{nm}^2+\Delta_{ma}^2)/2] \\ & \times\Bigg\{\sum_{l=0}^{\infty}\frac{\Gamma_{na}}{l![(\varepsilon_n/\overline{h}+l\omega-\omega_1-\omega_2)^2+\Gamma_{na}^2]} \\ & \times\Bigg|\sum_{j=0}^{l}\frac{l!(\Delta_{nm}/\sqrt{2})^j(\Delta_{ma}/\sqrt{2})^{l-j}}{j!(l-j)!} \\ & \times\sum_{k=0}^{\infty}\frac{(-1)^k(\Delta_{nm}\Delta_{ma}/2)^k}{k![i(\varepsilon_M/\overline{h}-\omega_1-j\omega+l\omega+k\omega)+\Gamma_{ma}]}\Bigg|^2 \\ & +\frac{(2\Gamma_{mm}-\Gamma_{mm})\Gamma_{ma}}{\Gamma_{mm}}\sum_{k=0}^{\infty}\frac{(\Delta_{ma}^2/2)^k}{k![(\varepsilon_m/\overline{h}+k\omega-\omega_1)^2+\Gamma_{ma}^2]}\sum_{j=0}^{k}\frac{k!(\Delta_{ma}^2/2)^j}{(k-j)!(j!)^2} \\ & \times\sum_{p=0}^{2j}\frac{(-1)^p(2j)!}{p!(2j-p)!}\sum_{l=0}^{\infty}\frac{(\Delta_{nm}^2/2)^l}{l!\{[(\varepsilon_n-\varepsilon_m)/\overline{h}-\omega_2+j\omega-p\omega+l\omega]^2+\Gamma_{mn}^2\}}\Bigg\} \end{aligned} \quad (1)$$

where, in the surrounding braces, the first part corresponds to the contribution of W_{sim}, and the second part to the contribution of W_{seq}. Suffixes a, m and n denote the initial, intermediate and final states of the transition. ε_n and ε_m are energy levels, ω_1 and ω_2 are the photon frequencies absorbed in TPA and E_1 and E_2 are the electric field strengths in the light beams at ω_1 and ω_2 in vacuum. ω is the vibrational frequency. Δ_{nm} and Δ_{ma} represent the dimensionless displacements between the equilibrium points of the intermediate and final states, and the intermediate and initial states, respectively. In equation (1), Γ_{ij} is referred to as the dephasing constant related to the states (i and j). In other words, Γ_{ij} is the interval between the centre frequency at the maximum transition intensity and the frequency at half-maximum intensity. From the viewpoint of spectroscopy, it means the Lorentzian half-width at half-maximum (HWHM) breadth of the transition between the related states. In this equation, the population decay constant Γ_{mm} of the intermediate state has the same order of magnitude and unit as those of Γ_{ma}. Γ_{mm} can be set to be equal to the value of Γ_{ma}.

Utilizing the Judd–Ofelt theory [19, 20], the module square of electric dipole transition moment $|M_{ij}|^2$ between the states i and j within $4f^N$ configuration can be calculated by

$$|M_{ij}|^2 = \frac{1}{3}\frac{1}{2J+1}\,e^2\sum_{t=2,4,6}\Omega_t|U_{ij}^{(t)}|^2 \quad (2)$$

where the factor $1/3$ results from the average of directions, J is the total angular momentum quantum number of the initial state. In fact, $|M_{ij}|^2$ expressed in (2) represents the dipole moment between all the Stark levels of the ground state i (assuming all are equally populated) and the state j. Ω_t are the intensity parameters of the laser crystal, $U_{ij}^{(t)}$ are the reduced-matrix elements of the unit tensor operator $U^{(t)}$ of rank t between the states i and j. The parameters of Ω_2, Ω_4 and Ω_6 in Pr^{3+}:YAG are 0, 12.20×10^{-20} and 8.27×10^{-20} cm^2, respectively, measured by Malinowski *et al* [26]. The values of $|U_{ij}^{(t)}|^2$ for Pr^{3+} are obtained from [27]. The $4f\rightarrow5d$ inter-configurational transition moment can be estimated using the radial integral $\langle4f|r|5d\rangle$ which was calculated to be 0.778 atomic unit for the Pr^{3+} ion [28].

In addition, considering Lorentz-local-field correction for the electric field strength in the laser crystal [29], the refractive index factor $\chi = [(n_c^2+2)^2/(9n_c^2)]^2$ should be multiplied

into the transition probability expression, where n_c is the refractive index of the crystal and it changes with the incident wavelength [30].

According to the definition, the TPA cross section σ is written as [31]

$$\sigma = \frac{\hbar^2 \omega_1 \omega_2 W}{I_1 I_2} \tag{3}$$

where W is the TPA transition probability and I_1 and I_2 are the pumping laser intensities at ω_1 and ω_2, respectively. The unit of σ is cm^4 s. In air, light intensity I in (3) is proportional to the squares of the electric field strengths through the relation

$$I = \tfrac{1}{2}\varepsilon_0 c n_a |E|^2 \tag{4}$$

where E is the electric field strength of the light beam in a vacuum. ε_0 and c are the dielectric constant and the velocity of light in vacuum, respectively, and n_a is the refractive index of air. When the TPA probability W is written as the form $\chi |E_1|^2 |E_2|^2 W'$, the TPA cross section σ in the laser crystal can be expressed as

$$\sigma = \frac{2\hbar^2 \omega_1 \omega_2 \chi W'}{\pi \varepsilon_0^2 n_a^2 c^3}. \tag{5}$$

Because of the independence on the pumping laser intensities, the cross section is more suitable to be used to describe the TPA processes than the transition probability.

Table 1. Values of parameters used to calculate the resonant TPA cross sections for transitions from the ground state to the second excited state of the 4f5d configuration in Pr^{3+}:YAG with equations (1) and (5); see text for identification of constants.

Constant	Value	Reference
Γ_{ma}	85.5 cm^{-1}	[13]
Γ_{na}	6575 cm^{-1}	[13]
Γ_{mn}	6575 cm^{-1}	[13]
Γ_{mm}	85.5 cm^{-1}	[13]
ω	350 cm^{-1}	[33]
Δ_{ma}	0.32	[33]
Δ_{nm}	3.54	[33]

To calculate the TPA cross section using equations (1) and (5), the values of parameters Γ_{ij}, Γ_{mm}, ω and Δ_{ij} are required. For resonant TPA transitions in Pr^{3+}:YAG under study, all these values are listed in table 1. The HWHM linewidth Γ_{ij} can be determined directly from the data of linewidth in [13], measured by Xie *et al* by one-photon absorption spectrum. In rare earth ion doped laser crystals, because of the strong coupling of electron–phonon, the radiationless phonon transition will interfere with TPA processes and, in particular, the sequential TPA processes. Moreover, unlike the case of atom, the electron transition between two states of a doped ion in laser crystals, especially the inter-configuration transition, may cause a change of distance between the ion and the ligand. These two kinetic effects will make to some extent impacts on TPA in crystals. As can be seen in equation (1), the parameters related to the two processes, i.e. the vibrational frequency and the dimensionless displacement, are involved in the density matrix TPA theory. In the single vibrational mode approximation, the vibrational frequency ω corresponds to the effective frequency of phonons in the crystal [32, 33]. For the 4f $\rightarrow$ 5d transition in Pr^{3+}:YAG, $\omega = 350$ cm^{-1} [33]. The typical values of the dimensionless displacements Δ_{ma} and Δ_{nm} for Pr^{3+}:YAG are, respectively, 0.32 and 3.54, which are determined from the literature [33] on the assumption that the effective degenerate factor of the effective phonon mode is unity.

3. Results and discussion

Making use of values of parameters given above and equations (1) and (5), we calculate resonant TPA cross sections for transitions from the ground state to the second 4f5d state in Pr^{3+}:YAG. The calculated TPA cross sections together with corresponding experimental results are presented in table 2. In order to understand clearly the contributions of simultaneous and sequential terms, their respective cross sections are also listed in this table. As can be seen from table 2, most values of total cross section calculated are in good agreement with those determined experimentally. For example, the peak TPA cross section actually measured at the excitation energy of 22 123 cm^{-1} is found to be 4.0×10^{-50} cm^4 s [13] and our theoretical value is 2.75×10^{-50} cm^4 s. Compared with the theoretical result 0.8×10^{-50} cm^4 s also estimated by Xie *et al* [13] in terms of the standard second-order perturbation description, it is obvious that the density matrix TPA theory employed in this paper can very well reproduce the experimental results. For another higher peak cross section at the excitation energy of 20 503 cm^{-1}, the calculated value 3.17×10^{-50} cm^4 s is in much closer agreement to the measured value 3.8×10^{-50} cm^4 s.

Table 2. Calculated cross sections of resonant two-photon transitions from the ground state to the second excited 4f5d state in Pr^{3+}:YAG and comparison with previous experimental results.

		Calculated cross section			Experimental
Intermediate state	Energy (cm^{-1})	Simultaneous (10^{-50} cm^4 s)	Sequential (10^{-50} cm^4 s)	Total (10^{-50} cm^4 s)	cross section [13] (10^{-50} cm^4 s)
$^3P_0$	20 503	1.06	2.11	3.17	3.8
	20 554	1.07	2.12	3.19	3.0
$^3P_1 + {}^1I_6$	20 816	0.43	0.86	1.29	0.5
	21 005	0.44	0.87	1.31	1.2
	21 057	0.44	0.88	1.32	1.8
	21 134	0.44	0.88	1.33	1.4
	21 691	0.47	0.93	1.40	1.7
	21 884	0.48	0.95	1.43	1.2
$^3P_2$	22 123	0.92	1.83	2.75	4.0
	22 311	0.93	1.86	2.80	1.6
	22 588	0.96	1.91	2.87	0.9

In addition, it is shown in table 2 that the simultaneous and sequential TPA cross sections offer basically close contributions to the total cross section for the resonant case as conforming to the indication given by Fujimura and Lin [24]. In our calculations, it is found that the ratio of simultaneous to sequential contributions is mainly dependent on the two parameters Γ_{na} and Γ_{mn}. Due to the specific data of these parameters in the problem, the ratio is approximately 0.5, which can be seen directly from table 2.

The YAG crystal has a cubic space-group O_h^{10} symmetry. The Pr^{3+} dopant ions substitute for Y^{3+} ions in point-group D_2 symmetry sites [34]. According to the group theory, the $^3P_1$ and $^1I_6$ manifolds split three and thirteen Stark levels, respectively, the positions of which were determined by Malinnowski *et al* [35]. In the TPA experiment of Xie *et al* [13], just six resonant TPA peaks are found to belong to the intermediate state $^3P_1 + {}^1I_6$. Of them there are at least three peaks resonating with the $^1I_6$ intermediate state. When the values of $|U_{ij}^{(t)}|^2$ (see equation (2)) related to the $^1I_6$ state are used, the calculated values of the six TPA cross sections, as shown in table 2, are all very consistent with the measured values. By comparison, if using the values of $|U_{ij}^{(t)}|^2$ related to the $^3P_1$ state, the six calculated data,

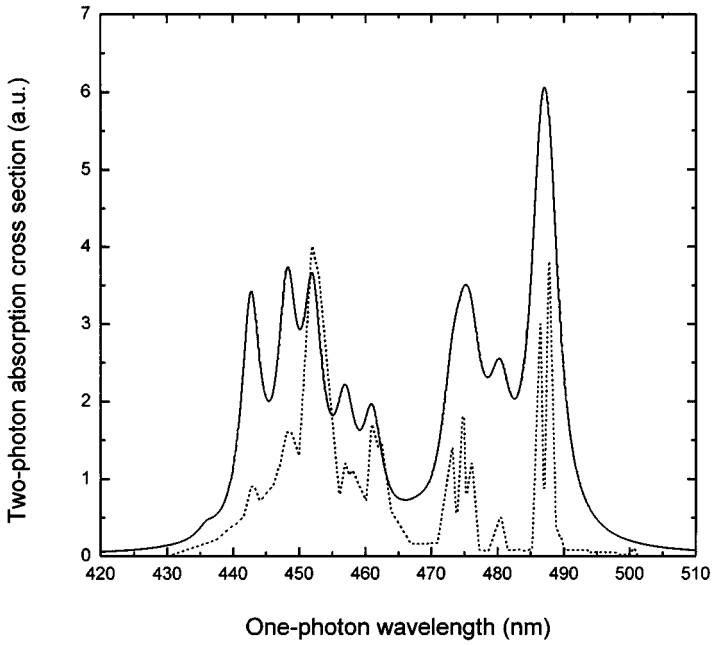

Figure 1. Composite graph of curves of calculated total cross section for two-photon absorption transitions resonating with eleven Stark levels split from the ^3P_J ($J = 0, 1, 2$) and $^1I_6$ intermediate states listed in table 2 and the corresponding experimental spectrum measured in [13]. The full curve denotes the calculated curve and the broken curve denotes the experimental spectrum.

which are in the range of 3.23×10^{-50}–3.58×10^{-50} cm^4 s, involve much larger deviations from the experimental data. Based on our theoretical results, therefore, it can be inferred that all of the six TPA peaks involving in the $^3P_1$ + $^1I_6$ state observed in the experiment [13] are actually resonant with the Stark levels of the $^1I_6$ manifold. This needs further experimental verification.

The Stark splitting is caused by the crystal-field interaction [36]. So, in order to minutely investigate the relative values of TPA cross sections resonating with Stark levels split from the same manifold, that is to much more accurately reproduce the experimental results listed in table 2, the crystal-field correction should be added to the density matrix TPA theory used in this paper. The reason for larger deviations between the theoretical and the experimental TPA cross sections at 20 816, 22 311 and 22 588 cm^{-1} is not explicit yet. Perhaps it is due to characteristics of crystal-field in Pr^{3+}:YAG.

In the region of 420–510 nm (19 603–23 810 cm^{-1}) of excitation wavelength, the composite graph of curves of calculated total cross section for TPA transitions resonating with eleven Stark levels listed in table 2 is presented in figure 1. For comparison, the experimental TPA spectrum measured in [13] in the same region of wavelength is also shown in this figure. Because the density matrix TPA theory employed here is much more applicable to the case of resonance than to the non-resonant case, some peak values at the resonant intermediate state energies as shown in figure 1 are influenced by the addition of a non-resonant cross section with larger computational errors. Hence, they are higher than the calculated and experimental data listed in table 2. However, it can be distinctly seen that the outline of the theoretical composite graph is basically consistent with that of the experimental TPA spectrum.

4. Conclusions

In this paper, the density matrix resonant two-photon absorption theory applicable to laser crystals doped with rare earth ions has been described. As an example, the resonant TPA cross sections for transitions from the ground state to the second excited state of the 4f5d configuration in Pr^{3+}:YAG are numerically calculated by using this theory. For the TPA peak cross section, the calculated value 2.75×10^{-50} cm^4 s is very consistent with the experimental value 4×10^{-50} cm^4 s. The good agreement of the calculated data with the measured values demonstrates that the density matrix resonant TPA theory, in which the phonon frequency and the dimensionless displacement between the ion and the ligand caused by the lattice vibration are considered, can predict resonant TPA cross sections much better than the standard second-order two-photon theory. The density matrix resonant TPA theory is a powerful and simple theoretical tool to seek upconversion laser based on TPA processes in laser crystals.

Acknowledgment

This work was financially supported by the National Natural Science Foundation of China under grant No 29871029.

References

[1] Pollack S A and Chang D B 1988 *J. Appl. Phys.* **64** 2885
[2] Ter-Mikirtychev V V and Tsuboi T 1995 *Phys. Rev.* B **52** 15 027
[3] Kaiser W and Garrett C G B 1961 *Phys. Rev. Lett.* 7 2529
[4] Auzel F E 1973 *Proc. IEEE* **61** 758
[5] Pollack S A, Chang D B and Moise N L 1986 *J. Appl. Phys.* **60** 4077
[6] Takahashi M, Shojiya M, Kanno R and Kawamoto Y 1997 *J. Appl. Phys.* **81** 2940
[7] Xie P and Rand S C 1992 *Opt. Lett.* **17** 1198
[8] Ju J J, Kwan T Y, Yun S I, Cha M and Seo H J 1996 *Appl. Phys. Lett.* **69** 1358
[9] Riedener T, Egger P, Hulliger J and Güdel H U 1997 *Phys. Rev.* B **56** 1800
[10] He G S, Yuan L, Cui Y C, Li M and Prasad P N 1997 *J. Appl. Phys.* **81** 2529
[11] Smart R G, Hanna D C, Tropper A C, Davey S T, Carter S F and Szebesta D 1991 *Electron. Lett.* **27** 1307
[12] Gayen S K, Xie B Q and Cheung Y M 1992 *Phys. Rev.* B **45** 20
[13] Xie B Q, Cheung Y M and Gayen S K 1993 *Phys. Rev.* B **47** 5557
[14] Gayen S K and Hamilton D S 1983 *Phys. Rev.* B **28** 3706
[15] Dagenais M, Downer M, Neumann R and Bloembergen N 1981 *Phys. Rev. Lett.* **46** 561
[16] Downer M C, Bivas A and Bloembergen N 1982 *Opt. Commun.* **41** 335
[17] Chase L L and Payne S A 1986 *Phys. Rev.* B **34** 8883
[18] Loudon R 1983 *The Quantum Theory of Light* (Oxford: Oxford University Press) ch 9
[19] Judd B R 1962 *Phys. Rev.* **127** 750
[20] Ofelt G S 1962 *J. Chem. Phys.* **37** 511
[21] Axe J D Jr 1964 *Phys. Rev.* **136** A42
[22] Gayen S K, Hamilton D S and Bartram R H 1986 *Phys. Rev.* B **34** 7517
[23] Judd B R and Pooler D R 1982 *J. Phys. C: Solid State Phys.* **15** 591
[24] Fujimura Y and Lin S H 1981 *J. Chem. Phys.* **74** 3726
[25] Lin S H, Fujimura Y, Neusser H J and Schlag W E 1984 *Multiphoton Spectroscopy of Molecules* (Orlando, FL: Academic) ch 2, 5; and references therein
[26] Malinowski M, Wolski R and Wolinski W 1990 *Solid State Commun.* **74** 17
[27] Carnall W T, Fialds P R and Rajnak K 1968 *J. Chem. Phys.* **49** 4424
[28] Carnall W T, Beitz J V and Crosswhite H 1983 *Systematics and Properties of Lanthanides* ed S P Sinha (Hingham: Kluwer) p 424
[29] Bartolo B D 1968 *Optical Interactions in Solid* (New York: Wiley) p 406
[30] Lomheim T S and DeShazer L G 1979 *Phys. Rev.* B **20** 4343
[31] Shen Y R 1984 *The Principles of Nonlinear Optics* (New York: Wiley) ch 18

[32] Fong F K and Wassam W A 1973 *J. Chem. Phys.* **58** 956
[33] Lauer H A and Fong F K 1974 *J. Chem. Phys.* **60** 274
[34] Gruber J B, Hills M E, Macfarlane R M, Morrison C A and Turner G A 1989 *Chem. Phys.* **134** 241
[35] Malinowski M, Joubert M F and Jacquier B 1994 *Phys. Rev.* B **50** 12 367
[36] Wybourne B G 1965 *Spectroscopic Properties of Rare Earths* (New York: Wiley) ch 6